Surfactant-promoted novel reductive synthesis of supported metallic Cu nanoclusters and their catalytic performances for selective dehydrogenation of methanol†

Rajaram Bal, Mizuki Tada and Yasuhiro Iwasawa*

Received (in Cambridge, UK) 7th April 2005, Accepted 28th April 2005
First published as an Advance Article on the web 9th June 2005
DOI: 10.1039/b504649a

We have found a surfactant-promoted novel reductive synthesis of metallic Cu nanoclusters on metal oxides under hydrothermal synthesis conditions, which are active for the selective dehydrogenation of methanol.

Effective ways to prepare supported nano-sized metal particles have been extensively explored as a key issue to develop new efficient catalytic systems.[1–4] The preparation of supported nanoparticles of novel metals by using appropriate zero-valent precursors[5,6] is established, while for late transition metals it is hard to prepare their metallic nanoparticles without reducing reagents because the larger oxophilicity and stronger interaction with the oxide supports lead to the formation of oxidic species and the uncontrollable decomposition and agglomeration of precursors cause undesired heterogeneous particle growth.

Hydrothermal synthesis in the presence of suitable surfactants promotes the organized assembly of cationic metal precursors to result in formation of well-structured oxide materials such as mesoporous alumina[7–14] and silica.[15] However, the surfactants themselves cannot reduce the cationic metal precursors to metallic nanostructures. Indeed, nickel[16,17] and copper[18] nanoparticles were synthesized in the presence of a surfactant, where hydrazine was used as a reducing reagent in an aqueous solution. There are no reports on spontaneous production of supported metallic nanoparticles under hydrothermal conditions in the presence of a surfactant. In this paper, we report a new way to prepare supported nano-sized metallic Cu clusters by using the surfactant and their catalytic performances for selective methanol dehydrogenation.

The typical preparation of Mo-oxide-supported metallic Cu nanoclusters is described as follows. An aqueous solution of a given amount of $Cu(NO_3)_2{\cdot}3H_2O$ was added dropwise with vigorous stirring to $(NH_4)_6Mo_7O_{24}{\cdot}4H_2O$ dissolved in hot distilled water. Then an aqueous solution of CTAB was added to the mixture of two metal precursors (Cu : CTAB : water = 1 : 0.75 : 300 molar ratio). After stirring until a homogeneous solution was obtained, the resultant mixed species was hydrothermally treated at 448 K for 24 h in a Tefron-lined autoclave vessel under an autogenous pressure. The product was washed with distilled water and ethanol, and dried at ambient temperature for 10 h and at 373 K for 8 h, followed by heating at 773 K for 6 h under a He flow (30 ml min^{-1}). The obtained samples were denoted as Cu/Mo-CTAB-(Cu wt%). A Cu/Mo sample was also prepared in the absence of CTAB (Cu/Mo-8.7). The hydrothermal synthesis of the Cu precursor alone or the Mo precursor alone in the presence of CTAB was also performed (Cu-CTAB and Mo-CTAB). $Zn(NO_3)_2{\cdot}6H_2O$, $Si(OC_2H_5)_4$, and $Al_2(SO_4)_3{\cdot}14$–$17H_2O$ were used as precursors for Zn, Si, and Al oxides, respectively. Supported Cu catalysts prepared as references by a conventional impregnation method are denoted as Cu/metal oxide-IMP-(Cu wt%). A Cu/Mo sample was also prepared by a coprecipitation method.

The Cu $2p_{3/2}$ binding energies in the XPS spectra for the prepared Cu nanoclusters, which were referred to the C 1s peak at 284.6 eV, were 932.4, 932.5, 932.5, and 932.4 eV for Cu/Mo-CTAB-3.1, Cu/Zn-CTAB-3.7, Cu/Si-CTAB-4.3, and Cu/Al-CTAB-5.3, respectively, which are similar to that for Cu metal. However, there is no difference in the Cu 2p binding energies between metallic Cu (932.3 eV) and Cu_2O (932.3 eV),[19] while the binding energy for CuO is as high as 933.8 eV.[19] Thus the XPS spectra indicate that the Cu^{2+} ions are reduced to Cu^0 or Cu^{1+} states by the hydrothermal treatment without reducing reagent.

The powder XRD patterns are shown in Fig. 1. All XRD peaks for Cu/Mo-CTAB-3.1 (Fig. 1(d)) are attributed to those for crystalline MoO_2 (Fig. 1(j)). The result of XRD was also confirmed by Mo K-edge EXAFS data. For the higher Cu loading sample (Cu/Mo-CTAB-7.8 (Fig. 1(e))), the small XRD peaks at 43.28° and 50.46° were observed and assigned as the Cu(111) and Cu(200) peaks, respectively.[20] On the other hand, the XRD pattern of Cu/Mo-8.7 prepared without CTAB (Fig. 1(f)) exhibited non-uniform phases, which is entirely different from that of Cu/Mo-CTAB-7.8 (Fig. 1(e)) with a similar Cu loading. The BET surface area estimated by nitrogen adsorption at 77 K for Cu/Mo-CTAB-3.1 was 1.4 $m^2\ g^{-1}$, suggesting a highly crystalline structure of the material. A TEM photograph depicts an aspect of the stacking of MoO_2 along the *c*-axis (Supporting Information 1†). The stacked crystalline MoO_2 merges to larger stacked particles, where Cu species are dispersed (Supporting Information 1†). In the absence of a pair of metal precursors, CuO (Cu-CTAB) and amorphous Mo oxides (Mo-CTAB) were obtained, respectively (Fig. 1(c) and (i)).

In the case of Cu/Zn-CTAB-3.7, highly crystalline ZnO (surface area: 1.4 $m^2\ g^{-1}$) was produced as shown in Fig. 1(l). On the other hand, Cu/Si-CTAB-4.3 showed no sharp XRD peaks for crystalline SiO_2 (Fig. 1(m)) and a high surface area of 204 $m^2\ g^{-1}$. The amorphous SiO_2 is characterized by a Si 2p peak of 103.4 eV and an O 1s peak of 532.9 eV. There were small peaks attributed to Cu metal on these samples.

Detailed structural parameters of the Cu species were obtained by Cu K-edge EXAFS analysis. The curve-fitting results are

† Electronic supplementary information (ESI) available: TEM and SEM photgraphs, and HCHO yields and selectivities for Cu nanoclusters. See http://www.rsc.org/suppdata/cc/b5/b504649a/

*iwasawa@chem.s.u-tokyo.ac.jp

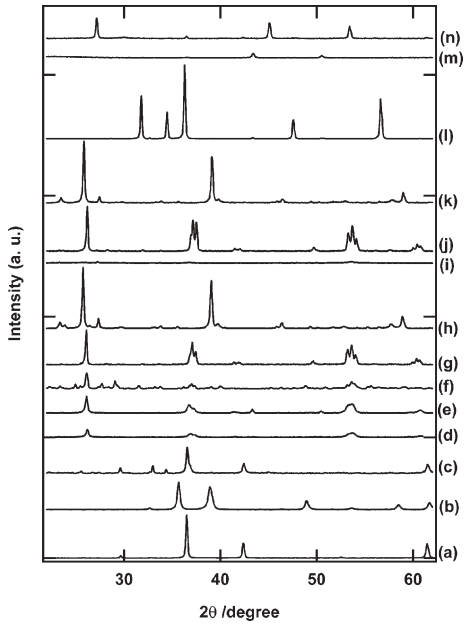

Fig. 1 XRD spectra for supported Cu catalysts, Cu oxides, and Mo oxides. (a) CuO, (b) Cu_2O, (c) Cu-CTAB, (d) Cu/Mo-CTAB-3.1, (e) Cu/Mo-CTAB-7.8, (f) Cu/Mo-8.7, (g) Cu/MoO_2-IMP-5.0, (h) Cu/MoO_3-IMP-5.0, (i) Mo-CTAB, (j) MoO_2, (k) MoO_3, (l) Cu/Zn-CTAB-3.7, (m) Cu/Si-CTAB-4.3, and (n) Cu/Al-CTAB-5.3.

summarized in Table 1. All EXAFS spectra were measured at 20 K without exposing to air. For all the samples prepared in the presence of CTAB, metallic Cu–Cu bonds were observed and there was no Cu–O bond. The Cu–Cu coordination number (CN) in fresh Cu/Mo-CTAB-3.1 was 4.4 ± 0.8 and the Cu–Cu distance was 0.254 ± 0.001 nm, which is similar to the bond length for Cu metal. The much smaller CN of Cu than in bulk Cu metal (CN = 12) indicates the formation of nano-sized metallic Cu clusters. Increasing the Cu loading did not increase the CN significantly (Cu/Mo-CTAB-7.8: CN = 4.5 ± 0.5). The metallic Cu clusters were stable as suggested by the CN of 3.9 ± 0.7 after catalytic methanol dehydrogenation at 523 K (Table 1). The CN of about four for Cu/Mo-CTAB-3.1 corresponds to the Cu CN of an octahedral Cu_6 cluster framework. On the other hand, Cu/Mo-8.7 prepared without the surfactant was characterized by Cu–O bonds (CN = 2.4 ± 0.3 and distance = 0.190 ± 0.002 nm) and there was no metallic Cu–Cu bonding as shown in Table 1. It is to be noted that the surfactant CTAB promoted the formation of metallic Cu nanoclusters in the Cu/Mo samples without any reducing reagent. However, $Cu(NO_3)\cdot 2H_2O$ was converted not to metallic Cu but to CuO under the hydrothermal conditions in the presence of CTAB when $(NH_4)_6Mo_7O_{24}\cdot 4H_2O$ was absent as above mentioned. Thus both the surfactant and the Mo precursor are indispensable for the formation of metallic Cu nanoclusters from the Cu^{2+} precursor. The CTAB decomposes to NH_3/NH_4OH under the hydrothermal conditions at 773 K. The Mo precursor in an organized assembly produced by CTAB may enhance the decomposition of CTAB to NH_3/NH_4OH, which may reduce the Cu^{2+} species under the hydrothermal conditions at 448 K.

Table 1 The curve-fitting results of Cu K-edge EXAFS measured at 20 K

Sample	Shell	CN	Distance/nm	σ^2/ 10^{-5} nm^2
Cu/Mo-CTAB-3.1 (fresh)[a]	Cu–Cu	4.4 ± 0.8	0.254 ± 0.001	3 ± 1
(after reaction)[b]	Cu–Cu	3.9 ± 0.7	0.254 ± 0.001	2 ± 1
Cu/Mo-CTAB-7.8 (fresh)[c]	Cu–Cu	4.5 ± 0.5	0.254 ± 0.001	4 ± 1
Cu/Mo-8.7 (fresh)[d]	Cu–O	2.4 ± 0.3	0.190 ± 0.002	8 ± 2
Cu/Zn-CTAB-3.7 (fresh)[e]	Cu–Cu	6.0 ± 1.3	0.257 ± 0.001	4 ± 1
(after reaction)[f]	Cu–Cu	8.8 ± 0.7	0.254 ± 0.001	4 ± 1
Cu/Si-CTAB-4.3 (fresh)[g]	Cu–Cu	4.4 ± 0.7	0.254 ± 0.001	4 ± 1
Cu/Al-CTAB-5.3 (fresh)[h]	Cu–Cu	1.5 ± 0.2	0.249 ± 0.001	4 ± 1

[a] k = 30–120 nm^{-1}, R = 0.18–0.28 nm, ΔE_0 = 2 ± 2 eV, R_f = 1.29%. [b] k = 30–120 nm^{-1}, R = 0.18–0.28 nm, ΔE_0 = 4 ± 2 eV, R_f = 0.95%. [c] k = 30–140 nm^{-1}, R = 0.18–0.28 nm, ΔE_0 = 3 ± 1 eV, R_f = 0.78%. [d] k = 30–114 nm^{-1}, R = 0.10–0.20 nm, ΔE_0 = −1 ± 3 eV, R_f = 1.94%. [e] k = 30–114 nm^{-1}, R = 0.18–0.28 nm, ΔE_0 = 8 ± 3 eV, R_f = 1.27%. [f] k = 30–114 nm^{-1}, R = 0.18–0.28 nm, ΔE_0 = 2 ± 1 eV, R_f = 0.17%. [g] k = 30–140 nm^{-1}, R = 0.18–0.28 nm, ΔE_0 = 3 ± 2 eV, R_f = 1.89%. [h] k = 30–140 nm^{-1}, R = 0.16–0.27 nm, ΔE_0 = −5 ± 2 eV, R_f = 0.93%.

The hydrothermal synthesis with other pairs of precursors for supports in the presence of CTAB also produced nano-sized metallic Cu clusters with Cu–Cu bond distances of 0.249–0.257 nm. The CNs of Cu were 6.0 ± 1.3, 4.4 ± 0.7, and 1.5 ± 0.2 for Cu/Zn-CTAB-3.7, Cu/Si-CTAB-4.3, and Cu/Al-CTAB-5.3, respectively, as shown in Table 1. Average sizes of the metallic Cu nanoclusters are estimated to decrease in the order for the supports: ZnO > MoO_2 ≈ SiO_2 > Al_2O_3.

We have examined the catalytic performances of the prepared Cu nanoclusters for the selective dehydrogenation of methanol to form HCHO and H_2. The selective dehydrogenation of methanol was carried out in a fixed-bed flow type glass reactor (id 6 mm) at 523 K and a space velocity of 10 000 h^{-1}. The catalytic performances of the various Cu catalysts for methanol dehydrogenation are summarized in Table 2.

Cu/Mo-CTAB was the most active catalyst for HCHO formation: 61.2% and 81.3% conversion for Cu/Mo-CTAB-3.1 and Cu/Mo-CTAB-7.8, respectively. Selectivity towards HCHO was as high as 98.5% and no dehydration occurred, and as a result H_2 selectivity was 100% (Table 2). Metallic Cu nanoclusters on ZnO and SiO_2 also exhibited high selectivities of 99.1% and 87.9%, respectively for HCHO synthesis, whereas Cu/Al-CTAB-5.3 with the smaller CN and Cu–Cu bond distance (Table 1) was much less selective for HCHO (53.4%). This may be a distinct example of the structure-dependent catalytic aspect of dehydrogenation.

The metallic Cu nanoclusters in Cu/Mo-CTAB were durable under the methanol dehydrogenation at 523 K. The structural parameters determined by Cu K-edge EXAFS for Cu/Mo-CTAB-3.1 after the catalytic reaction indicate that there is no significant change in the structures of Cu nanoclusters during the catalysis (Table 1). The HCHO yield and selectivity were constant for at least 6 h (Supporting Information 2†). In the Cu/Zn-CTAB-3.7 sample, there was sintering of the Cu species during catalysis. The CN of Cu changed from 6.0 ± 1.3 (at 0.257 ± 0.001 nm) to 8.8 ± 0.7 (at 0.254 ± 0.001 nm) as shown in Table 1. The HCHO yield gradually decreased with an increase in the size of Cu clusters in the case of the Cu/Zn-CTAB catalyst (Supporting Information 2†).

Table 2 Catalytic performances of the supported nano-sized metallic Cu catalysts, impregnated Cu catalysts, Cu oxides, Mo oxides, and Zn oxide for methanol dehydrogenation[a]

Catalyst	Conversion (mol%)	Selectivity (C%)[b]				
		HCHO	CO	HCO_2CH_3	CH_3OCH_3	H_2[c]
Cu/Mo-CTAB-3.1	61.2	98.5	0.4	1.1	0	100
Cu/Mo-CTAB-7.8	81.3	88.9	7.6	3.5	0	100
Cu/Mo-8.7[d]	45.3	55.6	15.7	28.7	0	100
Cu/Zn-CTAB-3.7	26.5	99.1	0.5	0.4	0	100
Cu/Si-CTAB-4.3	8.7	87.9	3.9	8.2	0	100
Cu/Al-CTAB-5.3	38.3	53.4	40.8	1.8	4.0	98.6
Cu-CTAB	9.2	47.3	50.1	2.6	0	100
Cu_2O	7.4	26.9	26.7	18.6	27.8	87.7
CuO	5.6	29.1	32.1	16.3	22.5	90.7
MoO_2	3.2	22.3	24.2	14.9	38.6	81.6
MoO_3	2.9	36.5	12.9	13.9	36.7	80.6
ZnO	1.2	12.9	45.3	8.4	33.4	87.0
Cu/MoO_2-IMP-5.0	12.3	51.2	17.4	5.5	25.9	87.6
Cu/MoO_2-IMP-5.0[e]	17.4	54.1	21.6	17.9	6.4	97.3
Cu/Mo-COPRE-7.2[e]	27.1	43.0	28.4	11.9	16.7	93.0
Cu/ZnO-IMP-5.0	2.3	41.3	15.3	7.5	35.9	81.6
Cu/SiO_2-IMP-10.0	9.5	45.6	4.5	20.3	29.6	83.5

[a] Catalyst: 0.20 g, GHSV (gas-hourly space velocity): 10 000 h^{-1}, 523 K, CH_3OH : He: 10 : 90 (mol%), time on stream: 30 min. [b] Selectivity (C%) = (products (C base)/consumed methanol (C base)) × 100. [c] H_2 selectivity (mol%) = (formed H_2/mol)/(formed H_2 + formed H_2O)/mol) × 100. [d] Prepared without CTAB. [e] Reduced with H_2 at 773 K before use as catalyst.

The effect of the surfactant CTAB on the catalyst preparation was significant. Cu/Mo-8.7 prepared without CTAB exhibited much lower methanol conversion (45.3%) and HCHO selectivity (55.6%) compared to 81.3% and 88.9%, respectively for Cu/Mo-CTAB-7.8 prepared with CTAB. Further the Cu/Mo-8.7 sample produced a significant amount of HCO_2CH_3 (28.7%). The Cu species in Cu/Mo-8.7 are oxidized as above mentioned (Table 1), which is in contrast to the formation of metallic Cu nanoclusters in Cu/Mo-CTAB. The impregnated catalysts, Cu/MoO_2-IMP-5.0, Cu/ZnO-IMP-5.0, and Cu/SiO_2-IMP-10.0 were also much less active and less selective as shown in Table 2. H_2 selectivities on these catalysts were less than 90%. Cu-CTAB (mainly CuO), MoO_2, and ZnO did not show significant performances either (Table 2). Even when the Cu species of Cu/MoO_2-IMP-5.0 and Cu/Mo-COPRE-7.2 were reduced with H_2, the catalytic performances were not improved (Table 2). It is to be noted that the metallic Cu nanoclusters with CNs of 4–6 hydrothermally synthesized in the presence of CTAB possess tremendous catalytic performances for methanol dehydrogenation.

In conclusion, we have found a surfactant-promoted novel reductive synthesis of metallic Cu nanoclusters on inorganic oxides for the first time. The hydrothermal treatment of a mixture of Cu nitrate and some metal precursors in the presence of a surfactant CTAB produced metallic Cu nanoclusters on metal oxides, characterized by XRF, XPS, XRD, EXAFS, and BET. In the cases of Mo and Zn, highly crystalline oxides were produced. In the absence of CTAB, no metallic Cu species were produced. The metallic Cu nanoclusters may be formed in the organized assembly composed of the Mo precursor and the surfactant under the hydrothermal synthesis conditions. The MoO_2-supported metallic Cu nanoclusters were the most active and selective for methanol dehydrogenation.

We thank Prof. S. Namba at Teikyo University of Science and Technology for SEM and TEM measurements. R. B. thanks the Japan Society for the Promotion of Science (JSPS) for a fellowship. The XAFS measurements were performed with the approval of PAC (proposal No.: 2003G092).

Rajaram Bal, Mizuki Tada and Yasuhiro Iwasawa*
Department of Chemistry, Graduate School of Science, The University of Tokyo, Hongo, Bunkyo-ku, Tokyo, 113-0033, Japan.
E-mail: iwasawa@chem.s.u-tokyo.ac.jp; Fax: +81-3-5800-6892;
Tel: +81-3-5841-4363

Notes and references

1 M. J. Boudart, *J. Mol. Catal.*, 1985, **30**, 27.
2 R. Schlöegl and S. B. Abd Hamid, *Angew Chem., Int. Ed.*, 2004, **43**, 1628.
3 A. T. Bell, *Science*, 2003, **299**, 1688.
4 B. F. G. Johnson, *Top. Catal.*, 2003, **24**, 147.
5 P. D. Nellist and S. J. Pennycook, *Science*, 1996, **274**, 413.
6 B. C. Gates, *J. Mol. Catal. A: Chem.*, 2000, **163**, 55.
7 S. A. Bagshaw and T. J. Pinnavaia, *Angew. Chem., Int. Ed. Engl.*, 1996, **35**, 1102.
8 F. Vaudry, S. Khodabandeh and M. E. Davis, *Chem. Mater.*, 1996, **8**, 1451.
9 M. Yada, M. Machida and T. Kijima, *Chem. Commun.*, 1996, 769.
10 S. Cabrera, J. E. Haskouri, H. Alamo, A. Beltran, D. Beltran, S. Mendioroz, M. D. Marcos and D. Amoros, *Adv. Mater.*, 1999, **11**, 379.
11 S. Velange, J.-L. Guth, F. Kolenda, S. Lacombe and Z. Gabelica, *Microporous Mesoporous Mater.*, 2000, **35–36**, 597.
12 H. Y. Zhu, J. D. Riches and J. C. Barry, *Chem. Mater.*, 2002, **14**, 2086.
13 Z. Zhang, R. W. Hicks, T. R. Pauly and T. J. Pinnavaia, *J. Am. Chem. Soc.*, 2002, **124**, 1592.
14 S. Lee, C. Fan, T. Wu and S. L. Anderson, *J. Am. Chem. Soc.*, 2004, **126**, 5682.
15 Y. Han and J. Y. Ying, *Angew. Chem., Int. Ed.*, 2005, **44**, 288.
16 D.-H. Chen and C.-H. Hsieh, *J. Mater. Chem.*, 2002, **12**, 2412.
17 S.-H. Wu and D.-H. Chen, *Chem. Lett.*, 2004, **33**, 406.
18 S.-H. Wu and D.-H. Chen, *J. Colloid Interface Sci.*, 2004, **273**, 165.
19 B. R. Strohmeier, D. E. Leyden, R. S. Field and D. M. Hercules, *J. Catal.*, 1985, **94**, 514.
20 P. H. Matter, D. J. Braden and U. S. Ozkan, *J. Catal.*, 2004, **223**, 340.